

Computational search for Dirac materials in f -electron antiperovskites

Anna Pertsova,¹ R. Matthias Geilhufe,¹ Martin Bremholm,^{2,3} and Alexander V. Balatsky^{1,4}

¹*Nordita, KTH Royal Institute of Technology and Stockholm University,
Roslagstullsbacken 23, SE-106 91 Stockholm, Sweden*

²*Department of Chemistry and iNANO, Aarhus University, 8000 Aarhus, Denmark*

³*Center for Materials Crystallography, Aarhus University, 8000 Aarhus, Denmark*

⁴*Dept of Physics, University of Connecticut, Storrs, CT 06269, USA*

(Dated: February 19, 2019)

We present the result of an *ab initio* search for new Dirac materials among inverse perovskites. Our investigation is focused on the less studied class of lanthanide antiperovskites containing heavy f -electron elements in the cation position. Some of the studied compounds have not yet been synthesized experimentally. Our computational approach is based on density functional theory calculations which account for spin-orbit interaction and strong correlations of the f -electron atoms. We find several promising candidates among lanthanide antiperovskites which host bulk Dirac states close to the Fermi level. Specifically, our calculations reveal massive three-dimensional Dirac states in materials of the class A_3BO , where $A=Sm, Eu, Gd, Yb$ and $B=Sn, Pb$.

I. INTRODUCTION

Dirac materials (DMs) is a growing class of materials which exhibit a linear, Dirac-like spectrum of quasi-particle excitations [1]. Examples of DMs that have attracted particular attention in the past decade include graphene [2], three-dimensional (3D) topological insulators (TIs) [3, 4], topological crystalline insulators (TCIs) [5], and the newly discovered three-dimensional DMs such as Dirac [6] and Weyl semimetals [7, 8]. Over the past several years, it has been suggested that a new subclass of DMs can be found in cubic antiperovskite materials [9–13]

Antiperovskites, or inverse perovskites, are inorganic compounds with a perovskite type structure in which the positions of cations and anions are interchanged. The typical structure is A_3BX , where A is an electropositive cation, B is a divalent metallic anion and X is a monovalent anion i.e. the position of A and X are reversed compared to ordinary perovskites. Antiperovskites have a great potential for electronic, magnetic and thermoelectric applications [14].

Regarding the search for DMs, much focus has been on antiperovskite oxides with a simple cubic structure, A_3BO , where A is an alkaline earth metal such as Ca, Ba, Sr . The prototypical example is Ca_3PbO which was proposed as a potential DM in a number of studies [10–13]. Recently, superconductivity has been reported in a similar compound, the antiperovskite Dirac-metal oxide Sr_3SnO with hole doping [15]. There has been an increasing interest in other antiperovskite materials. A group of nitride antiperovskites with a common structure A_3BiN , where $A=Ca, Ba, Sr$ has been predicted to be 3D TIs when subject to properly designed uniaxial strain [10]. A recent density functional theory (DFT) based study of a larger class of alkaline earth pnictides A_3BX , where $A=Ca, Ba, Sr$ and $B, X=N, P, As, Sb, Bi$ found several materials that can be driven into topological phases by properly engineered strain [16]. A promising candidate is Ca_3BiP which is a topological semimetal without strain

but can be driven into a 3D TI or a Dirac semimetal phase.

The nature of the Dirac states in antiperovskite materials predicted so far has been studied from different viewpoints. Initially, the data mining search based on electronic structure calculations performed in Ref. [9] identified Ca_3PbO (and similar compounds, A_3BO , $A=Ca, Ba, Sr$ and $B=Sn, Pb$) as a possible 3D TI. More specifically, it was suggested to be a strong 3D TI based on apparent band inversion at the Γ point. The band inversion was confirmed in other studies [10, 12, 17]. However, despite the band inversion, the product of parities of the bands at time-reversal invariant momenta remains the same with or without spin orbit coupling (SOC). Therefore, based on the parity criterion [18], strain free Ca_3PbO is a trivial insulator. Properly engineered uniaxial strain can change the ordering of the inverted bands, turning the material into a 3D TI, similarly to Ca_3BiN [10]. In the absence of strain, the Ca_3PbO family was predicted to be TCI with unusual surface states with open Fermi surface similar to Weyl semimetals [12, 13]. At the same time, it was suggested that Ca_3PbO is a massive 3D DM, with Dirac nodes occurring in the 3D Brillouin away from any high-symmetry point [11, 17, 19–21].

In fact, the topological gap at Γ and the 3D Dirac states away from Γ may coexist in these materials. Based on topological band theory, Hsieh *et al.* [12] showed that the band inversion at the Γ point, responsible for the TCI phase in Ca_3PbO , leads to the appearance of a gapped node (avoided crossing) along the Γ - X direction of the 3D Brillouin zone. This feature was studied in detail by Kariyado and Ogata [11, 17] using a combination of *ab initio* and tight-binding methods. In particular, it was shown that these states can be described as massive Dirac fermions. Photoemission experiments are required to verify these theoretical predictions.

More recent theoretical work has predicted the existence of Dirac nodal lines in materials with weak SOC, which can be realized in some antiperovskite compounds [22, 23]. Specifically, Yu *et al.* [22] found that in

the absence of SOC, Cu_2PdN is a nodal-line semimetal with three nodal circles due to cubic symmetry. Nodal lines originate from the band inversion at the R point of the 3D Brillouin zone and are protected by time reversal and inversion symmetries [24]. Inclusion of SOC drives the system into a Dirac semimetal phase with three pairs of Dirac nodes. Similar conclusions were found by Kim *et al.* [23] for a more general case of Cu_2N doped with non-magnetic transition metal atoms, i.e. in $\text{Cu}_3\text{X}_x\text{N}$ (antiperovskite structure) with $\text{X}=\text{Ni}, \text{Cu}, \text{Zn}, \text{Pd}, \text{Ag}, \text{Cd}$. In particular, two maximally-doped cases, Cu_3PdN and Cu_3ZnN were studied with effective Hamiltonian and *ab initio* methods, demonstrating bulk Dirac nodal lines and nearly-flat surface states.

We note that the existence of nodal lines is not a universal property of antiperovskites. Since it requires vanishing or weak spin-orbit interaction, it is not realized in compounds containing elements with very large atomic numbers. On the other hand, band inversion at time reversal invariant momenta and the occurrence of nodes along adjacent symmetry lines is a common feature. Unlike in 3D TIs, the band inversion in antiperovskites is not due to SOC but can be induced by changing the lattice constant or the chemical elements. The details of the electronic structure, such as the character of the inverted bands and the position of the Dirac nodes are material specific.

In this work we focus on the scarcely studied group of lanthanide antiperovskite oxides, A_3BO , where $\text{A}=\text{Sm}, \text{Eu}, \text{Gd}, \text{Yb}$ and $\text{B}=\text{Sn}, \text{Pb}$. Among published work, Yb_3SnO and Yb_3PbO were predicted to be 3D TIs [9]. Based on electronic structure calculations, we find that this group of compounds is characterized by massive Dirac nodes in the 3D Brillouin zone. The most interesting candidates are Eu_3SnO , Eu_3PbO , Yb_3SnO and Yb_3PbO which have Dirac states near the Fermi level. Among these materials, Yb_3PbO is the most promising for further studies and applications since the Dirac states are isolated from other bands. The origin of the 3D Dirac states is similar to the case of Ca_3PbO . Our DFT calculations show that most of the considered lanthanide antiperovskites possess a finite magnetic moment due to unpaired f -electrons in their outer shells. This offers intriguing possibilities of combining magnetism and Dirac fermion physics in pristine materials without doping or proximity effects.

The paper is organized as follows. In Sec. II we provide computational details. Section III reports the outcome of our *ab initio* search for DMs among lanthanide antiperovskites. Namely, we summarize the results of electronic structure calculations for the materials of this class in the bulk phase. Several candidates displaying Dirac states are identified. The electronic structure of the most promising candidates with isolated Dirac cones near the Fermi level are discussed in more detail. We also analyze the character and the possible origin of the Dirac states using a specific example of Yb_3PbO . Finally, we draw some conclusions in Sec. IV.

II. METHODS

We performed DFT calculations using the full-potential all-electron linearized augmented plane-waves method as implemented in the Wien2k *ab initio* package [25]. The Perdew-Burke-Ernzerhof generalized gradient approximation (PBE-GGA) [26] is used for the exchange correlation functional. For lanthanide antiperovskites, the GGA+U method was used to account for local correlations at the cation site. We choose $U=7$ eV in our calculations which is within the commonly accepted range for rare earths [27]. We used 126 non-equivalent k -points in a $10 \times 10 \times 10$ mesh of the first Brillouin zone for self-consistent calculations. SOC is included in all calculations as it can not be ignored in heavy-element compounds.

Geometry optimization was performed to find the equilibrium lattice constant, which is particularly important for compounds for which no experimental structural data is available (Sm_3SnO , Sm_3PbO , Gd_3SnO , Gd_3PbO). The results of structural (volume) optimization together with experimental (estimated or observed) lattice constants for lanthanide antiperovskites are presented in Table I. For compounds that have been synthesized and for which structural data can be found in the literature (Eu_3SnO , Eu_3PbO , Yb_3SnO , Yb_3PbO), the DFT optimized lattice constants are close to experimental values. We use experimental lattice parameters [28, 29] for the existing lanthanide antiperovskites, as well for the test data set of alkali antiperovskites [29, 30].

TABLE I. Experimental and DFT optimized lattice constant for lanthanide antiperovskite oxides: A_3BO , $\text{A}=\text{Sm}, \text{Eu}, \text{Gd}, \text{Yb}$, and $\text{B}=\text{Sn}, \text{Pb}$; space group $\text{P}\bar{m}3\text{m}$. E(O) refers to estimated (observed) structural data. References are given for the experimental lattice constants.

System	Experiment, a (\AA)	DFT, a (\AA)
Sm_3SnO	5.111 (E)	4.984
Sm_3PbO	5.124 (E)	5.015
Eu_3SnO	5.077 (O) [29]	5.018
Eu_3PbO	5.091 (O) [29]	5.051
Gd_3SnO	5.043 (E)	4.851
Ga_3PbO	5.058 (E)	4.887
Yb_3SnO	4.837 (O) [28]	4.804
Yb_3PbO	4.859 (O) [28]	4.842

III. RESULTS AND DISCUSSION

We use the well studied Ca_3PbO group of antiperovskite oxides containing alkali metals as a test set for our *ab initio* search. The results are summarized in Table II [see also the electronic structure for Ca_3PbO in Fig. 2(a,b)]. The table includes information on the presence (+) or absence (-) of Dirac nodes according to

our DFT electronic structure calculations, as well as the availability of structural data (synthesis), and references to previous theoretical work with a brief note on the predicted character of the Dirac states.

Our results for the Ca_3PbO family are in agreement with Kariyado and Ogata [11]. Namely, we find gapped nodes formed by linearly dispersing bands along the Γ - X direction in all compounds of this group. The nodes are located at the Fermi level. In Ba_3SnO and Ba_3PbO , there are other states crossing the Fermi level thus obscuring the Dirac states. The results also largely agree with Hsieh *et al.* [12], with the possible exception of Ca_3SnO .

TABLE II. Possible Dirac materials in antiperovskite oxides with alkali metals: A_3BO , $\text{A}=\text{Ca}$, Ba , Sr , $\text{B}=\text{Sn}$, Pb ; space group $\text{P}\bar{m}3\text{m}$.

System	DM	Synthesis	Theory
Ba_3PbO	+	[28–30]	[9](3DTI), [10](3DTI+strain), [11](3DDM), [12](TCI)
Ba_3SnO	-	[28–30]	[9–12]
Ca_3PbO	+	[28–30]	[9](3DTI), [10](3DTI+strain), [11](3DDM), [12](TCI)
Ca_3SnO	+	[28–30]	[9](3DTI), [11](3DDM), [12](TCI)
Sr_3PbO	+	[28–30]	[9](3DTI), [10](3DTI+strain), [11](3DDM), [12](TCI)
Sr_3SnO	+	[28–30]	[9](3DTI), [12](TCI)

We now focus on lanthanide antiperovskite oxides. The results of the electronic structure calculations for this group of materials are summarized in Table III, where we also include the information on the value of the calculated magnetic moment (for lanthanide atoms in the unit cell). The available experimental and theoretical literature is considerably more scarce compared to the Ca_3PbO family. Structural data is available for Eu_3BO and Yb_3BO ($\text{B}=\text{Sn}$, Pb), while for Sm_3BO and Gd_3BO ($\text{B}=\text{Sn}$, Pb), we use the lattice constant obtained from DFT (see Table I). We note that Yb_3BO ($\text{B}=\text{Sn}$, Pb) was classified as a potential TI by Klintonberg *et al.* [9].

Our calculations reveal gapped 3D Dirac nodes in Eu_3SnO , Eu_3PbO , Yb_3SnO and Yb_3PbO along the Γ - X direction of the 3D Brillouin zone. The calculated bandstructures of these materials are presented in Fig. 1. Based on bulk electronic structure, we conclude that Eu_3BO and Yb_3BO ($\text{B}=\text{Sn}$, Pb) are 3D DMs with a finite Dirac gap. The energy gap at the node is $\Delta \approx 25$ meV for Eu_3BO ($\text{B}=\text{Sn}$, Pb), $\Delta \approx 30$ meV for Yb_3SnO and $\Delta \approx 50$ meV for Yb_3PbO . In the case of Eu_3BO ($\text{B}=\text{Sn}$, Pb), there are other bands present at the Fermi level. In Eu_3PbO , the gapped Dirac node is located at the Fermi level, while in Eu_3SnO it is located 100 meV below the Fermi level. The case of Yb_3PbO is particularly interesting as it has an isolated Dirac node at the Fermi level.

We find that Eu_3SnO and Eu_3PbO are magnetic with a total magnetic moment of $\approx 21 \mu_B$ and a magnetic moment on Eu site of $\approx 6.9 \mu_B$. Yb_3SnO and Yb_3PbO do

TABLE III. Possible Dirac materials in lanthanide antiperovskite oxides: A_3BO , $\text{A}=\text{Sm}$, Eu , Gd , Yb , $\text{B}=\text{Sn}$, Pb ; space group $\text{P}\bar{m}3\text{m}$.

System	DM	Magnetic moment (μ_B)	Synthesis	Theory
Sm_3PbO	-	5.8	-	-
Sm_3SnO	-	5.7	-	-
Eu_3PbO	+	6.9	[28]	-
Eu_3SnO	+	6.9	[28]	-
Gd_3PbO	-	7.1	-	-
Ga_3SnO	-	7.2	-	-
Yb_3PbO	+	0	[29]	[9](3DTI)
Yb_3SnO	+	0	[29]	[9](3DTI)

not show any sizable magnetic moment (this is expected since Yb has a fully filled f -shell).

Finally, we comment on the possible origin of bulk Dirac states in these materials. For this we compare the character of the low energy states for the typical alkali antiperovskite oxide Ca_3PbO and a representative example of lanthanide antiperovskite oxides Yb_3PbO (see Fig. 2). It was noted in Refs. [11, 17] that the low energy Dirac states in Ca_3PbO are formed mainly by Ca $3d$ and Pb $6p$ orbitals. Among Ca $3d$, the $3d_{x^2-y^2}$ orbitals give the major contribution to the Dirac states. We have verified this picture [see the electronic structure of Ca_3PbO with band character in Fig. 2(a,b)].

Based on the insight from DFT electronic structure, Kariyado and Ogata [11, 17] constructed a tight-binding Hamiltonian with a basis formed by Ca $d_{x^2-y^2}$ and Pb p states, which the authors proved to be a Dirac Hamiltonian yielding 3D gapless Dirac states along the Γ - X line (there is a total of 6 nodes at equivalent points of the Brillouin zone due to cubic symmetry). It was suggested that a small gap at the Dirac node (few tens of meV's) is due to SOC and the coupling to other states away from the Fermi level i.e. Pb $5d$ and other Ca $3d$ states [17]. We have verified in our calculations that in the absence of SOC, the Dirac states are gapless. Further analysis of the DFT bands for Ca_3PbO with SOC reveals that the two bands forming the node along the Γ - X direction belong to the same irreducible representation, Γ_7 of the C_{4v} double point group [see Fig. 2(a,b)], which further justifies the avoided crossing between these bands (irreducible representation have been computed with Wien2k [25] and independently verified with QUANTUM ESPRESSO [31, 32]).

SOC is also responsible for the band inversion at the center of the Brillouin zone which was found in Ca_3PbO [11, 12, 17]. Since Ca d and Pb p states, which give rise to low-energy electronic states, have different parities, there exist two possible band orderings at the Γ point. In the normal ordering, the d orbitals of Ca (A position in A_3BO) lie above the Pb p orbitals (B position in A_3BO). However, in the presence of SOC the order is

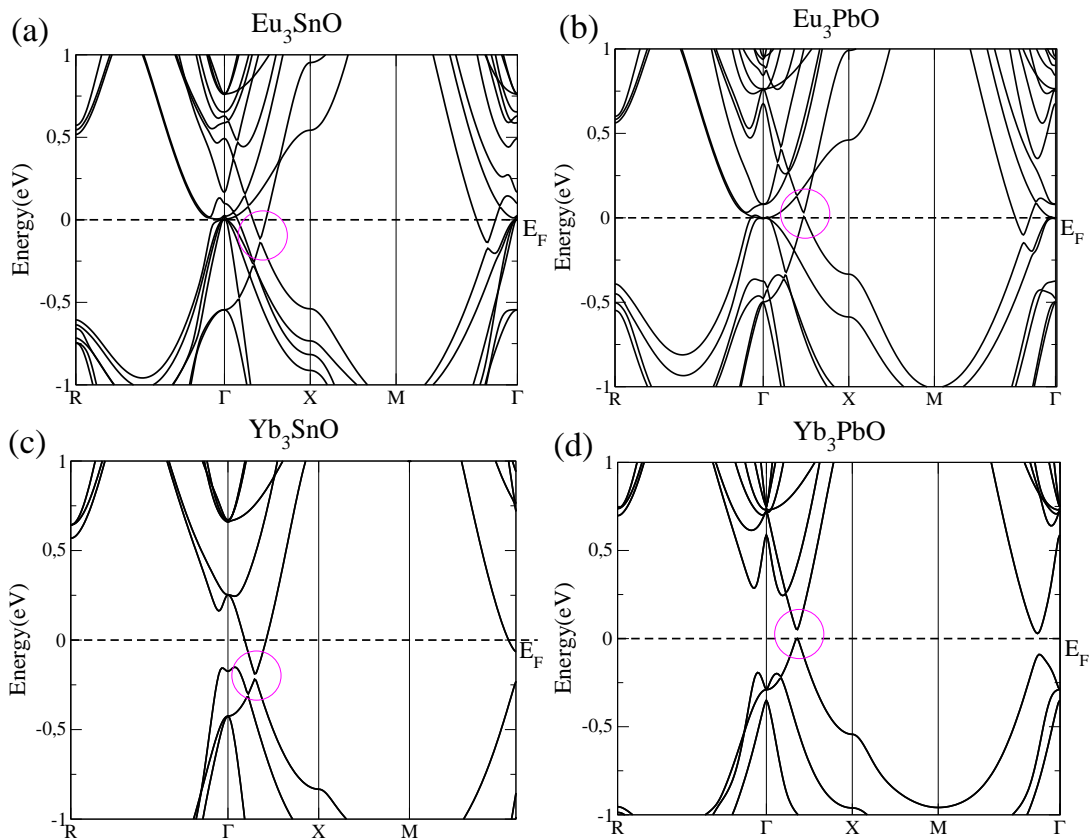


FIG. 1. Calculated bandstructures of cubic lanthanide antiperovskites (a) Eu_3SnO , (b) Eu_3PbO , (c) Yb_3SnO , and (d) Yb_3PbO . SOC is included in the calculations. The horizontal dashed line marks the position of the Fermi level. Circles highlight the massive Dirac fermion feature along the Γ - X direction.

reversed, namely the top of the p bands lies above the bottom of the d bands. This band inversion signals a possible topological phase which was detected by Klintenberg *et al.* [9]. However, it leaves the materials a trivial insulator in the Z_2 classification of TIs because the product of parity eigenvalues remains unchanged due to the four-fold degeneracy of valence and conduction band extrema at Γ [10, 17].

Nevertheless, the inverted band ordering is an important ingredient in the low-energy effective Hamiltonian of Ref. [17] which produces 3D Dirac states away from Γ . It was subsequently demonstrated by Hsieh *et al.* [12] that this band inversion leads a TCI phase described by a nonzero mirror Chern number. It was also shown that the bulk Dirac node is a direct consequence of the band inversion at Γ i.e. the band crossing on the Γ - X is absent in the trivial phase characterized by normal band ordering [12]. This is different from the band inversion at the R point in Cu_3PdN , which involves p and d states of the metallic anion (Pd $5p$ states are lower than Pd $4d$ states). When SOC is included, Cu_3PdN exhibits Dirac nodes along R - X and R - M directions, where the node along R - M remains gapless [22]. Similarly, the band inversion at X in Cu_3ZnN leads to nodes along R - X and R - M [23].

We find that the character of low energy states in Yb_3PbO is similar to Ca_3PbO [see Fig. 2(c,d)]. In this case, the Dirac states are formed mainly by Yb $4d_{x^2-y^2}$ and Pb $6p$ orbitals. The valence and conduction bands along Γ - X belong to the same irreducible representation, Γ_7 of the C_{4v} group. These are strong indications that the origin of the Dirac states in this material is similar to Ca_3PbO . Hence, we conclude that Yb_3PbO is characterized by massive 3D Dirac fermions at finite k and is also a potential TCI. Further theoretical and experimental work will be useful to describe bulk Dirac states and possible topological surface states due to the TCI phase in this material and other lanthanide antiperovskites with similar properties.

We also considered hypothetical structures A_3BO , $\text{A}=\text{Gd}, \text{Sm}$ and $\text{B}=\text{Sn}, \text{Pb}$, for which no experimental structural data is available to date. For these compounds, we have obtained DFT optimized crystal structures (see Table I), however their dynamic structural stability needs to be investigated further. Although our calculations showed interesting features, including band crossings near the Fermi level, we were not able to clearly identify 3D Dirac states in these compounds.

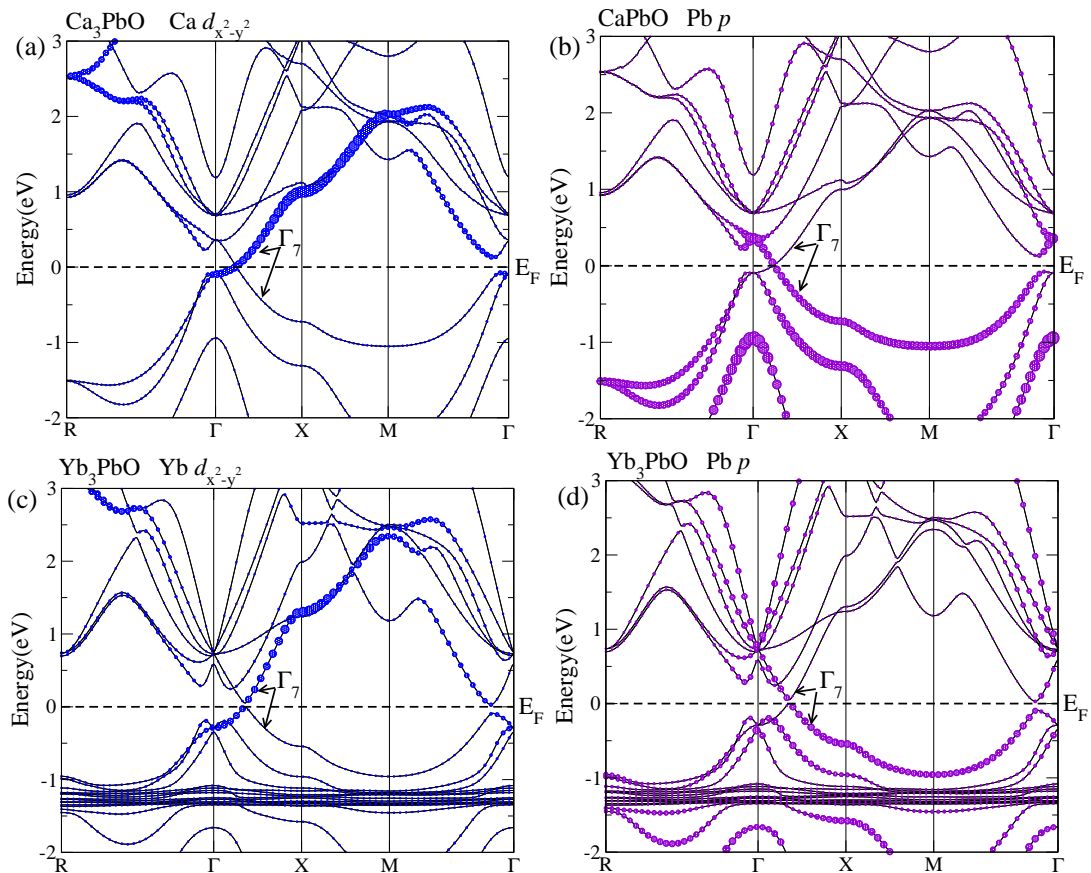


FIG. 2. Band character of cubic alkali antiperovskite (a,b) Ca_3PbO and lanthanide antiperovskite (c,d) Yb_3PbO . Filled circles show relative contributions of Ca and Yb d -states (a,c) and Pb p states (b,d). Only $d_{x^2-y^2}$ states are shown for Ca and Yb. We have verified that the contribution of other d orbitals with different symmetry is negligible at low energies. In panels (c) and (d), the highly localized states below the Fermi level are Yb $4f$ -states. The horizontal dashed line marks the position of the Fermi level. Irreducible representations are shown for valence and conduction bands along the Γ -X direction.

IV. CONCLUSION

In conclusion, we performed an *ab initio* search for Dirac materials among some antiperovskite oxides. Our data set includes both the Ca_3PbO family as a test subset and the less studied lanthanide antiperovskites containing f -electron elements, some of which have not been synthesized to date. For the Ca_3PbO family (A_3BO , $\text{A}=\text{Ca}$, Ba , Sr , $\text{B}=\text{Sn}$, Pb), our electronic structure calculations show gapped 3D Dirac states, which is consistent with previous theoretical work. Among the f -electron antiperovskites, we identify Eu_3BO and Yb_3BO ($\text{B}=\text{Sn}$, Pb) as 3D DMs, which display massive Dirac nodes along the Γ -X in the three-dimensional Brillouin zone. The nodes are energetically close to the Fermi level and the energy gap at the nodes is few tens of meV's. Yb_3PbO is particularly promising as it has an isolated Dirac node at the Fermi level. We find that in addition to hosting Dirac states, Eu_3SnO and Eu_3PbO display a finite magnetic moment. As demonstrated previously for Ca_3PbO family, the existence of bulk Dirac states at finite k is a direct

consequence of the band inversion at the center of the 3D Brillouin zone, which gives rise to a TCI phase. Hence, the 3D DMs found among the f -electron antiperovskites may be potential TCIs.

V. ACKNOWLEDGMENTS

We are grateful to P. Hofmann for useful discussion. This work was supported by the VILLUM FONDEN via the Centre of Excellence for Dirac Materials (Grant No. 11744), the European Research Council under the European Unions Seventh Framework Program (FP/2207-2013)/ERC Grant Agreement No. DM-321031, the Swedish Research Council Grant No. 638-2013-9243, and the Knut and Alice Wallenberg Foundation. The authors acknowledge computational resources from the Swedish National Infrastructure for Computing (SNIC) at the High Performance Computing Center North (HPC2N)

- [1] T. Wehling, A. M. Black-Schaffer, and A. V. Balatsky, *Advances in Physics* **63**, 1 (2014).
- [2] A. Castro Neto, F. Guinea, N. M. Peres, K. S. Novoselov, and A. K. Geim, *Rev. Mod. Phys.* **81**, 109 (2009).
- [3] M. Z. Hasan and C. L. Kane, *Rev. Mod. Phys.* **82**, 3045 (2010).
- [4] X.-L. Qi and S.-C. Zhang, *Rev. Mod. Phys.* **83**, 1057 (2011).
- [5] L. Fu, *Phys. Rev. Lett.* **106**, 106802 (2011).
- [6] M. Neupane, S.-Y. Xu, R. Sankar, N. Alidoust, G. Bian, C. Liu, I. Belopolski, T.-R. Chang, H.-T. Jeng, H. Lin, A. Bansil, F. Chou, and M. Z. Hasan, *Nature Communications* **5**, 3786 (2014).
- [7] S.-M. Huang, S.-Y. Xu, I. Belopolski, C.-C. Lee, G. Chang, B. Wang, N. Alidoust, G. Bian, M. Neupane, C. Zhang, S. Jia, A. Bansil, H. Lin, and M. Z. Hasan, *Nature Communications* **6**, 7373 (2015).
- [8] S.-Y. Xu, I. Belopolski, N. Alidoust, M. Neupane, G. Bian, C. Zhang, R. Sankar, G. C. Chang, Z. Yuan, C.-C. Lee, S.-M. Huang, H. Zheng, J. Ma, D. S. Sanchez, B. Wang, A. Bansil, F. Chou, P. P. Shibayev, H. Lin, S. J. Jia, and M. Z. Hasan, *Science* **349**, 613 (2015).
- [9] M. Klintonberg, J. Haraldsen, and A. Balatsky, *Applied Physics Research* **6** (2014).
- [10] Y. Sun, X.-Q. Chen, S. Yunoki, D. Li, and Y. Li, *Phys. Rev. Lett.* **105**, 216406 (2010).
- [11] T. Kariyado and M. Ogata, *Journal of the Physical Society of Japan* **80**, 083704 (2011), <http://dx.doi.org/10.1143/JPSJ.80.083704>.
- [12] T. H. Hsieh, J. Liu, and L. Fu, *Phys. Rev. B* **90**, 081112 (2014).
- [13] C.-K. Chiu, Y.-H. Chan, X. Li, Y. Nohara, and A. P. Schnyder, *Phys. Rev. B* **95**, 035151 (2017).
- [14] M. Bilal, S. Jalali-Asadabadi, R. Ahmad, and I. Ahmad, *Journal of Chemistry* **2015**, 495131 (2015).
- [15] M. Oudah, A. Ikeda, J. N. Hausmann, S. Yonezawa, T. Fukumoto, S. Kobayashi, M. Sato, and Y. Maeno, *Nat. Comm.* **7**, 13617 (2016).
- [16] W. F. Goh and W. E. Pickett, *Phys. Rev. B* **97**, 035202 (2018).
- [17] T. Kariyado and M. Ogata, *Journal of the Physical Society of Japan* **81**, 064701 (2012), <http://dx.doi.org/10.1143/JPSJ.81.064701>.
- [18] L. Fu and C. L. Kane, *Phys. Rev. B* **76**, 045302 (2007).
- [19] T. Kariyado, *Three-Dimensional Dirac Electron Systems in the Family of Inverse-Perovskite Material Ca_3PbO* (The University of Tokyo, 2012).
- [20] T. Kariyado, *Journal of Physics: Conference Series* **603**, 012008 (2015).
- [21] Y. Fuseya, M. Ogata, and H. Fukuyama, *Journal of the Physical Society of Japan* **81**, 013704 (2012), <http://dx.doi.org/10.1143/JPSJ.81.013704>.
- [22] R. Yu, H. Weng, Z. Fang, X. Dai, and X. Hu, *Phys. Rev. Lett.* **115**, 036807 (2015).
- [23] Y. Kim, B. J. Wieder, C. L. Kane, and A. M. Rappe, *Phys. Rev. Lett.* **115**, 036806 (2015).
- [24] H. Weng, Y. Liang, Q. Xu, R. Yu, Z. Fang, X. Dai, and Y. Kawazoe, *Phys. Rev. B* **92**, 045108 (2015).
- [25] P. Blaha, K. Schwarz, G. K. H. Madsen, D. Kvasnicka, and J. Luitz, *WIEN2K, An Augmented Plane Wave Plus Local Orbitals Program for Calculating Crystal properties* (Vienna University of Technology, Austria, 2001).
- [26] J. P. Perdew, K. Burke, and M. Ernzerhof, *Phys. Rev. Lett.* **77**, 3865 (1996).
- [27] D. van der Marel and G. A. Sawatzky, *Phys. Rev. B* **37**, 10674 (1988).
- [28] A. Velden and P. D. M. Jansen, *Journal of Inorganic and General Chemistry* **630**, 234 (2004).
- [29] J. Nuss, C. Mühle, K. Hayama, V. Abdolazimi, and H. Takagi, *Acta Cryst.* **B71**, 300 (2015).
- [30] A. Widera and H. Schäfer, *Materials Research Bulletin* **15**, 1805 (1980).
- [31] P. Giannozzi, S. Baroni, N. Bonini, M. Calandra, R. Car, C. Cavazzoni, D. Ceresoli, G. L. Chiarotti, M. Cococcioni, I. Dabo, A. D. Corso, S. de Gironcoli, S. Fabris, G. Fratesi, R. Gebauer, U. Gerstmann, C. Gougoussis, A. Kokalj, M. Lazzeri, L. Martin-Samos, N. Marzari, F. Mauri, R. Mazzarello, S. Paolini, A. Pasquarello, L. Paulatto, C. Sbraccia, S. Scandolo, G. Sclauzero, A. P. Seitsonen, A. Smogunov, P. Umari, and R. M. Wentzcovitch, *Journal of Physics: Condensed Matter* **21**, 395502 (2009).
- [32] P. Giannozzi, O. Andreussi, T. Brumme, O. Bunau, M. B. Nardelli, M. Calandra, R. Car, C. Cavazzoni, D. Ceresoli, M. Cococcioni, N. Colonna, I. Carnimeo, A. D. Corso, S. de Gironcoli, P. Delugas, R. A. D. Jr, A. Ferretti, A. Floris, G. Fratesi, G. Fugallo, R. Gebauer, U. Gerstmann, F. Giustino, T. Gorni, J. Jia, M. Kawamura, H.-Y. Ko, A. Kokalj, E. Kkbenli, M. Lazzeri, M. Marsili, N. Marzari, F. Mauri, N. L. Nguyen, H.-V. Nguyen, A. O. de-la Roza, L. Paulatto, S. Ponc, D. Rocca, R. Sabatini, B. Santra, M. Schlipf, A. P. Seitsonen, A. Smogunov, I. Timrov, T. Thonhauser, P. Umari, N. Vast, X. Wu, and S. Baroni, *Journal of Physics: Condensed Matter* **29**, 465901 (2017).